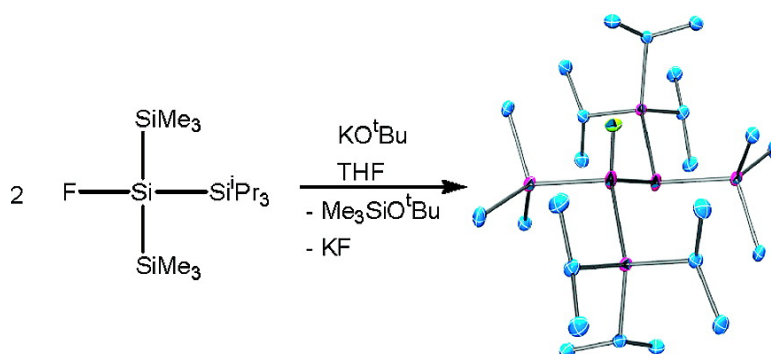


## Formation of Formal Disilene Fluoride Adducts

Michaela Zirngast, Michaela Flock, Judith Baumgartner, and Christoph Marschner

*J. Am. Chem. Soc.*, **2008**, 130 (51), 17460-17470 • DOI: 10.1021/ja805753d • Publication Date (Web): 02 December 2008

Downloaded from <http://pubs.acs.org> on February 8, 2009



### More About This Article

Additional resources and features associated with this article are available within the HTML version:

- Supporting Information
- Access to high resolution figures
- Links to articles and content related to this article
- Copyright permission to reproduce figures and/or text from this article

[View the Full Text HTML](#)

### Formation of Formal Disilene Fluoride Adducts

Michaela Zirngast, Michaela Flock, Judith Baumgartner, and Christoph Marschner\*

*Institut für Anorganische Chemie, Technische Universität Graz, Stremayrgasse 16,  
A-8010 Graz, Austria*

Received July 23, 2008; E-mail: christoph.marschner@tugraz.at

**Abstract:** Reactions of trisilylated silylfluorides with potassium *tert*-butoxide were found to give disilylated fluorosilylenoids. The latter undergo a self-condensation reaction, leading to the formation of  $\beta$ -fluorodisilanyl anions, which may also be considered as fluoride adducts of disilenes. The stereochemical outcome of this self-condensation depends on the bulkiness of the silyl substituents. Thus, mixtures of diastereomers are obtained in some cases. Reaction of a disilene adduct with magnesium bromide triggers metal fluoride elimination and formation of the respective tetrasilylated disilene. Attempts to exchange one silyl group of the starting material for a methyl, phenyl, or *tert*-butyl group led to a different course of reaction for the methyl and phenyl cases. The *tert*-butyl-substituted example gave the expected disilene adduct, but it was not the main product.

#### Introduction

Ever since the first synthesis of a disilene by West, Fink, and Michl,<sup>1</sup> this class of compounds has been the subject of enormous interest.<sup>2</sup> While the photochemical generation of silylenes and their subsequent dimerization to disilenes was the first known synthetic protocol, other methods such as reductive dehalogenation have been established in the meantime.<sup>2</sup> It is interesting to note that at about the same time as the first stable disilenes<sup>1,3</sup> were prepared, the first examples of stable silenes also were reported.<sup>4</sup> The more developed chemistry of carbon and the inherent asymmetry of silenes compared with disilenes, combined with different synthetic entries, brought it about that the structural variety of silenes was always more diverse than that of disilenes. Depending on substitution pattern and the method of synthesis, several different types of silenes (such as the Brook, the Ishikawa–Oehme–Apeloig, and the Wiberg silenes) can be distinguished. An especially interesting aspect about the Wiberg silenes that has been studied extensively<sup>5</sup> is the fact that these can be complexed with Lewis bases such as amines, ethers, and halides to form adducts. Among the bases

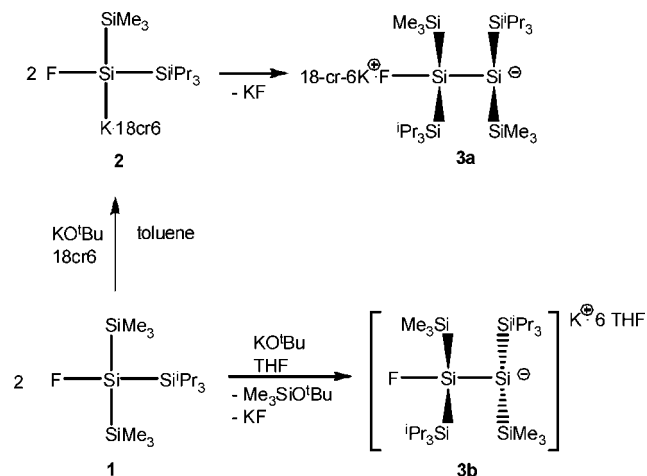
that have been used, fluoride and trimethylamine were found to exhibit the strongest degree of interaction. The adducts obtained have been used as “instant silenes” in cases where the noncomplexed silene was not stable. In one of his contributions<sup>5a</sup> on the topic, Wiberg offered the following speculation: *A prerequisite for adduct formation seems to be a polar Si=X double bond, as neither Brook’s sila enol ether,<sup>4a,6</sup> which has a largely nonpolar silicon–carbon double bond, nor West’s<sup>1</sup> or Masamune’s<sup>7</sup> (symmetrical) disilenes have been reported to form stable adducts.*

More recently, Tamao and Kawachi<sup>8</sup> introduced silylenoids,  $R_2Si(X)Li$  ( $X = NR_2, OR$ ), as a class of reactive silicon compounds having both electrophilic and nucleophilic character. By their very nature, these compounds (in the case of  $X = OR$ ) tend to undergo self-condensation, forming dimerization products of the type  $R_2XS_iSiR_2Li$ . During our own studies of the chemistry of polysilyl potassium compounds, it was found that the reaction of  $(Me_3Si)_3SiF$  with potassium *tert*-butoxide in an analogous way led to the formation of the  $\beta$ -fluorodisilanyl anion  $(Me_3Si)_2FSiSiK(SiMe_3)_2$ .<sup>9</sup> It was found that this compound is rather reluctant to eliminate potassium fluoride, thereby forming the respective disilene. This elimination reaction can, however,

- (1) West, R.; Fink, M. J.; Michl, J. *Science* **1981**, *214*, 1343–1344.
- (2) For the most recent review on disilenes, see: Kira, M.; Iwamoto, T. *Adv. Organomet. Chem.* **2006**, *54*, 73–148. For other reviews covering the field, see: (a) Weidenbruch, M. In *The Chemistry of Organic Silicon Compounds*; Rappoport, Z., Apeloig, Y., Eds.; Wiley: Chichester, U.K., 2001; p 391. (b) Kira, M. *Pure Appl. Chem.* **2000**, *72*, 2333–2342. (c) Okazaki, R.; West, R. *Adv. Organomet. Chem.* **1996**, *39*, 231–273. (d) Weidenbruch, M. *Coord. Chem. Rev.* **1994**, *130*, 275–300. (e) Lickiss, P. D. *Chem. Soc. Rev.* **1992**, *21*, 271–279. (f) West, R. *Pure Appl. Chem.* **1984**, *56*, 163–173. (g) Tokitoh, N. *Pure Appl. Chem.* **1999**, *71*, 495–502.
- (3) For another early disilene synthesis, see: Masamune, S.; Hanzawa, Y.; Murakami, S.; Bally, T.; Blount, J. F. *J. Am. Chem. Soc.* **1982**, *104*, 1150–1153.
- (4) (a) Brook, A. G.; Abdesaken, F.; Gutekunst, B.; Gutekunst, G.; Kallury, R. K. *J. Chem. Soc., Chem. Commun.* **1981**, 191–192. (b) Wiberg, N.; Wagner, G. *Angew. Chem.* **1983**, *95*, 1027–1028.
- (5) For example, see: (a) Wiberg, N.; Wagner, G.; Reber, G.; Riede, J.; Müller, G. *Organometallics* **1987**, *6*, 35–41. (b) Wiberg, N.; Köpf, H. *J. Organomet. Chem.* **1986**, *315*, 9–18. (c) Wiberg, N.; Joo, K.-S.; Polborn, K. *Chem. Ber.* **1993**, *126*, 67–69.

- (6) (a) Brook, A. G.; Nyburg, S. C.; Abdesaken, F.; Gutekunst, B.; Gutekunst, G.; Kallury, R. K. M. R.; Poon, Y. C.; Chang, Y.-M.; Wong-Ng, W. *J. Am. Chem. Soc.* **1982**, *104*, 5667–5672. (b) Nyburg, S. C.; Brook, A. G.; Abdesaken, F.; Gutekunst, G.; Wong Ng, W. *Acta Crystallogr.* **1985**, *C41*, 1632–1635.
- (7) Masamune, S.; Murakami, S.; Snow, J. T.; Tobita, H.; Williams, D. J. *Organometallics* **1984**, *3*, 333–334.
- (8) For Tamao and Kawachi’s seminal studies on silylenoids see: (a) Tamao, K.; Kawachi, A. *Angew. Chem., Int. Ed. Engl.* **1995**, *34*, 818–820. (b) Tanaka, Y.; Hada, M.; Kawachi, A.; Tamao, K.; Nakatsuji, H. *Organometallics* **1998**, *17*, 4573–4577. (c) Tamao, K.; Kawachi, A. *J. Am. Chem. Soc.* **1992**, *114*, 3989–3990. (d) Tamao, K.; Kawachi, A.; Tanaka, Y.; Ohtani, H.; Ito, Y. *Tetrahedron* **1996**, *52*, 5765–5772. (e) Tamao, K.; Kawachi, A. *J. Am. Chem. Soc.* **2000**, *122*, 1919–1926. (f) Kawachi, A.; Maeda, H.; Tamao, K. *Organometallics* **2002**, *21*, 1319–1321.
- (9) Fischer, R.; Baumgartner, J.; Kickelbick, G.; Marschner, C. *J. Am. Chem. Soc.* **2003**, *125*, 3414–3415.

**Scheme 1.** Reaction of **1** Leading Either to the Silylenoid **2**, Which Undergoes Self-Condensation to **3a**, or Directly to **3b** (Stereochemical Depiction Taken from Crystal Structure Analysis)



be induced by transmetalation reactions. A more covalent silicon–metal bond seems to facilitate the elimination.

In view of the similarity of the  $\beta$ -fluorodisilanyl anion to Wiberg's silene fluoride adducts, we believe that it is appropriate to regard  $(\text{Me}_3\text{Si})_2\text{FSiSiK}(\text{SiMe}_3)_2$  as the first example of a disilene adduct.

Although we have speculated that  $(\text{Me}_3\text{Si})_2\text{FSiSiK}(\text{SiMe}_3)_2$  is the product of self-condensation of the fluorosilylenoid  $(\text{Me}_3\text{Si})_2\text{Si}(\text{F})\text{K}$ , we were not able to prove the involvement of this intermediate. The principal existence of fluorosilylenoids was previously demonstrated by Wiberg.<sup>10</sup> A recent communication by Bravo-Zhivotovskii, Apeloig and co-workers<sup>11</sup> has even provided structural information. The current study explores the scope of the reaction of oligosilylfluorides with potassium *tert*-butoxide.

## Results and Discussion

**Disilene Adduct Formation.** In order to gain more information on the general nature of the reaction of oligosilyl fluorides with potassium alkoxides, it was decided to modify the substitution pattern of the starting material. Increasing the steric bulk around the central silicon atom by changing from  $(\text{Me}_3\text{Si})_3\text{SiF}$  to  $(\text{Me}_3\text{Si})_2(\text{iPr}_3\text{Si})\text{SiF}$  (**1**) suggested a more stable intermediate. Consistently, reaction of **1** with potassium *tert*-butoxide in the presence of 18-crown-6 in toluene allowed the NMR spectroscopic detection of the silylenoid  $(\text{Me}_3\text{Si})(\text{iPr}_3\text{Si})\text{Si}(\text{F})\text{K}$  (**2**) (Scheme 1). While it was reported that  $(\text{tert-Bu}_3\text{Si})_2\text{Si}(\text{F})\text{Li}$ , with its bulky *tert*-Bu<sub>3</sub>Si groups, required forcing conditions for self-condensation,<sup>11</sup> compound **2** underwent this process smoothly at ambient temperature to form what can be seen as the crown ether potassium fluoride adduct **3a** of the disilene  $(E)$ - $(\text{Me}_3\text{Si})(\text{iPr}_3\text{Si})\text{Si}=\text{Si}(\text{SiMe}_3)(\text{Si}^i\text{Pr}_3)$  (**4**) (Scheme 1).

When the reaction of **1** with potassium *tert*-butoxide was carried out in THF without crown ether, NMR spectroscopic observation of the intermediate silylenoid was not possible, and the related condensation product **3b** was isolated. This is in accordance with Tamao's results<sup>8a</sup> on silylenoids and with the reaction of  $(\text{Me}_3\text{Si})_3\text{SiOMe}$  with potassium *tert*-butoxide, which

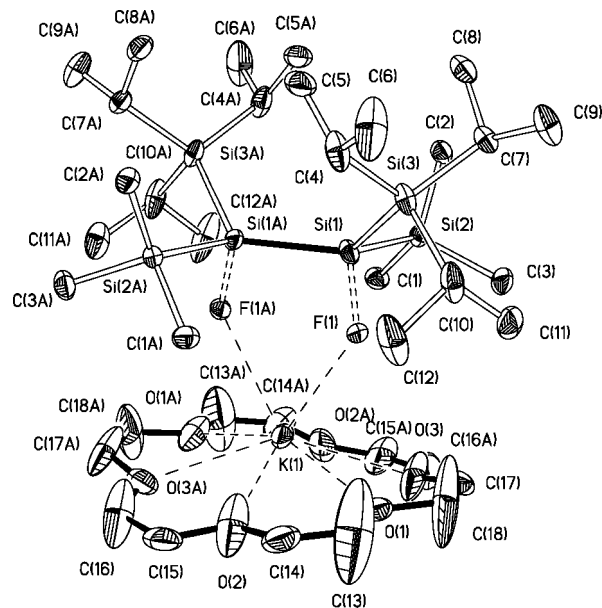


**Figure 1.** Molecular structure and numbering of **3a**. Selected bond lengths (Å) and bond angles (deg): F(1)–Si(1), 1.556(5); F(1)–K(1), 2.781(6); Si(1)–Si(1A), 2.321(3); Si(1)–Si(2), 2.355(2); Si(1)–Si(3), 2.364(2); Si(1)–F(1)–K(1), 131.9(3); F(1)–Si(1)–Si(2), 96.1(2); F(1)–Si(1)–Si(3), 108.8(2); Si(1A)–Si(1)–Si(3), 125.12(8); Si(2)–Si(1)–Si(3), 109.41(7).

led to the selective formation of the silylenoid  $(\text{Me}_3\text{Si})_2\text{Si}(\text{OMe})\text{K}$  in the presence of crown ether but gave the condensation product  $(\text{Me}_3\text{Si})_2(\text{MeO})\text{SiSi}(\text{SiMe}_3)_2\text{K}$  in THF.<sup>12</sup>

X-ray crystal structure analyses of **3a** and **3b** revealed that the former (Figure 1) is structurally related to  $(\text{Me}_3\text{Si})_2\text{FSiSiK}(\text{SiMe}_3)_2$ .<sup>9</sup> If the picture that considers these compounds to be formed by addition of a base to a disilene (Figure 4) is adopted, it can be said that the fluoride atom of **3a** coordinates to one of the formal disilene silicon atoms but is evenly distributed over the two possible sites, for which the expected occupation factor of 0.5 was observed.

In the case of  $(\text{Me}_3\text{Si})_2\text{FSiSiK}(\text{SiMe}_3)_2$ , interaction of the crown ether-coordinated potassium ion with the fluoride ion was observed only at one of the two possible sites.<sup>9</sup> For **3a**, a higher degree of symmetry was found, as the potassium ion resides at a central position so that it can interact to the same extent with the fluoride ion at either possible site (Figures 1 and 4).

The crystal structure of **3b** (Figure 2) shows it to be a separated ion pair. The potassium ion is coordinated by six THF molecules and thus is not able to engage in further interaction with the fluoride ion. Again, the fluoride is evenly distributed over two sites, coordinating to one of the two formal disilene atoms. In the case of **3b**, however, these positions are on different sides of the disilene plane (Figure 4).

It should be noted that the  $\beta$ -fluorodisilanyl anion units found in the two crystal structures are different stereoisomers. A Newman-type projection (Figure 3) shows that **3a** exhibits an eclipsed sawhorse conformation with the bulky triisopropylsilyl groups on different sides of the central bond. In contrast to this, **3b** features a staggered sawhorse conformation with the triisopropylsilyl groups in an *anti* arrangement.<sup>13</sup> If both conformations are brought to a Fischer-type projection, which requires

(10) (a) Wiberg, N.; Niedermayer, W. *J. Organomet. Chem.* **2001**, *628*, 57–64. (b) Wiberg, N.; Niedermayer, W.; Nöth, H.; Warchhold, M. *J. Organomet. Chem.* **2001**, *628*, 46–56.

(11) Molev, G.; Bravo-Zhivotovskii, D.; Karni, M.; Tumanskii, B.; Botoshansky, M.; Apeloig, Y. *J. Am. Chem. Soc.* **2006**, *128*, 2784–2785.

(12) Likhar, P. R.; Zirngast, M.; Baumgartner, J.; Marschner, C. *Chem. Commun.* **2004**, 1764–1765.

(13) Eliel, E. L.; Wilen, S. H.; Mander, L. N. *Stereochemistry of Organic Compounds*; Wiley-Interscience: New York, 1994.

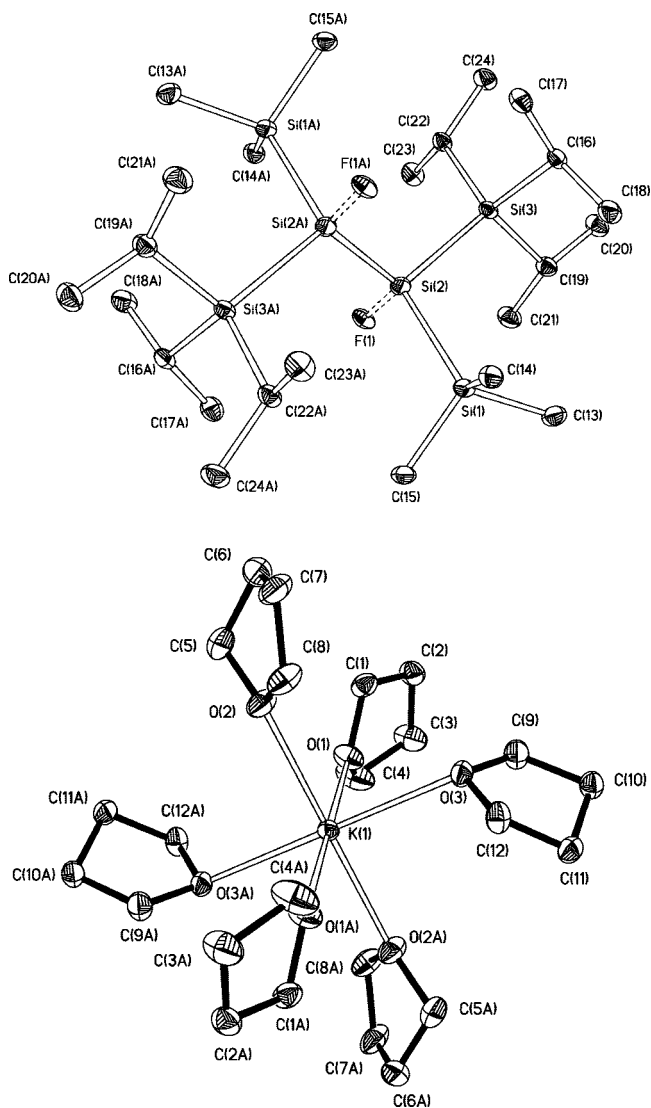


**Figure 2.** Molecular structure and numbering of **3b**. Selected bond lengths (Å) and bond angles (deg): Si(1)–Si(2), 2.3631(9); Si(2)–F(1), 1.492(2); Si(2)–Si(2A), 2.3285(13); Si(2)–Si(3), 2.3830(9); F(1)–Si(2)–Si(2A), 118.27(10); F(1)–Si(2)–Si(1), 104.44(9); Si(2A)–Si(2)–Si(1), 106.68(4); F(1)–Si(2)–Si(3), 105.30(9); Si(2A)–Si(2)–Si(3), 113.66(4); Si(1)–Si(2)–Si(3), 107.73(4).

rotation around the central bond for **3b**, it is clearly visible that they are different diastereomers (Figure 3). Using a Fischer-type description, we can assign them as pseudo-*threo* and -*erythro* configurations.

The description used for **3a** and **3b** refers to the situation in the crystal. In solution, the circumstances are likely to be different. Of particular importance for the solution case is the fact that the configuration of threefold-silylated silyl anions is not stable.<sup>14</sup> Inversion of configuration at the negatively charged silicon atom leads to interconversion of the two diastereomers. Nevertheless, the NMR spectra of both **3a** and **3b** show only one set of resonances in each case. This indicates that in solution only a single diastereomer (the more stable one) exists.

Attempts at further variation of the substituent pattern of the silyl fluorides provided insight into the steric interactions

between the silyl groups used. The reaction of  $(\text{Me}_3\text{Si})_2(\text{tert-BuMe}_2\text{Si})\text{SiF}$  (**5**) with potassium *tert*-butoxide gave the condensation product **6** as a 3:1 mixture of two diastereomers (Scheme 2). This shows that as the degree of steric interaction between the silyl groups is diminished, the energetically less favorable isomer becomes accessible under ambient conditions. Increasing the steric demand from *tert*-BuMe<sub>2</sub>Si to ThexMe<sub>2</sub>Si (**7**) increased the ratio of the two diastereomers of **8** to 6:1. We were also interested in obtaining disilene adducts with oligosilyl substituents, and therefore,  $(\text{Me}_3\text{Si})_2(\text{Me}_3\text{SiMe}_2\text{Si})\text{SiF}$  (**9**) was subjected to reaction with potassium *tert*-butoxide. The ratio of the observed diastereomers (**10**) was about 1:1, indicating not much difference in the steric demand of the trimethylsilyl and pentamethyldisilyl groups. The introduction of a larger oligosilyl residue, namely, the undecamethylcyclohexasilanyl unit in **11**, afforded the stereoselective formation of only one isomer of **12**. The steric bulk of the cyclohexasilanyl substituent was also sufficient to allow for the observation of the corresponding fluorosilylenoid  $(\text{Me}_{11}\text{Si}_6)(\text{Me}_3\text{Si})\text{Si(F)K}$  by means of <sup>19</sup>F NMR spectroscopy.

Having established the synthetic potential of the threefold-silyl-substituted silylfluorides for adduct formation, we were interested in the reactivity of similar compounds bearing one nonsilyl substituent. In a first attempt,  $(\text{Me}_3\text{Si})_2\text{MeSiF}$  (**13**) was reacted with potassium *tert*-butoxide. After the typical reaction time of 3 h,  $(\text{Me}_3\text{Si})_2\text{MeSiK}$ <sup>15</sup> was observed as the major product (Scheme 3). No sign of the typical Si–F coupling pattern of a disilene adduct could be detected in the <sup>29</sup>Si NMR spectrum. Repeating the reaction with  $(\text{Me}_3\text{Si})_2\text{PhSiF}$  (**14**) gave essentially the same result, with  $(\text{Me}_3\text{Si})_2\text{PhSiK}$ <sup>27</sup> being the major product. Monitoring of the reaction using <sup>29</sup>Si NMR spectroscopy provided evidence that the first step in both cases was nucleophilic attack of the potassium alkoxide at the central silicon atom accompanied by potassium fluoride elimination (Scheme 3).

The picture improved when the *tert*-butyl-substituted fluoride **15** was used. While the same reaction course as for the methyl- and phenyl-substituted compounds could be observed to some extent, some of the expected disilene fluoride adduct **16** was also formed (Scheme 4). Only one diastereomer was observed. In view of the steric bulk of the *tert*-butyl group, this seems reasonable. The formation of **16** indicates that the side reaction generating the silyl ether (Scheme 3) and subsequently the silyl anion may not only be caused by improved steric accessibility but also has electronic reasons.

**Disilene Formation and Reactivity.** The reactions of  $(\text{Me}_3\text{Si})_2\text{FSiSiK}(\text{SiMe}_3)_2$  with magnesium bromide and several other metal halides led to the elimination of metal fluoride and the release of tetrakis(trimethylsilyl)disilene.<sup>9</sup> As this compound is not stable at ambient temperature, it either underwent a [2 + 2] cycloaddition process to yield octakis(trimethylsilyl)cyclooctasilane or could be trapped with anthracene or 2,3-dimethylbutadiene. Analogously, the reactions of **3a** and **3b** with magnesium bromide led to the formation of the corresponding disilene **4**. Again, the triisopropylsilyl group proved to be a good choice, as the added steric bulk was sufficient to give a stable disilene. Probably because of the sterically more advantageous arrangement, only the *E* isomer of **4** was formed (Scheme 5).

While we have referred to the self-condensation products of the fluorosilylenoids as disilene adducts, one has to be aware of the fact that this is a formal description. In order to obtain

(14) (a) Flock, M.; Marschner, C. *Chem.—Eur. J.* **2002**, *8*, 1024–1030. (b) Fischer, R.; Marschner, C. In *Organosilicon Chemistry V*; Auner, N., Weis, J., Eds.; Wiley-VCH: Weinheim, Germany, 2003; pp 190–194.

(15) Marschner, C. *Eur. J. Inorg. Chem.* **1998**, 221–226.



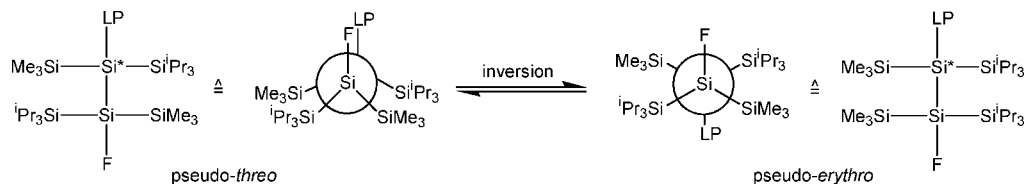


**Figure 3.** Graphical representations of the two diastereoisomers **3a** (left) and **3b** (right) found in the crystal, using Newman- and Fischer-type projections (LP = lone pair).

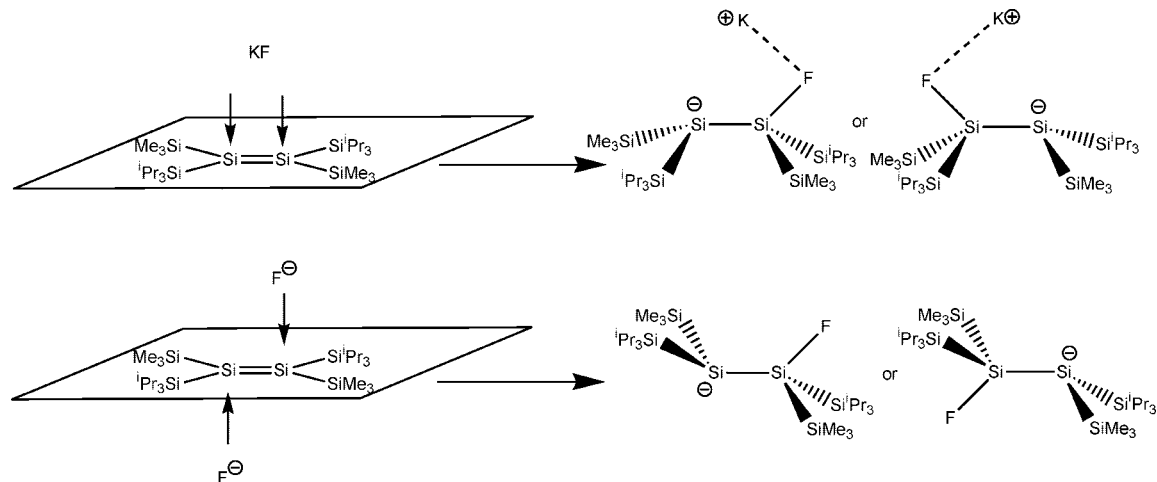
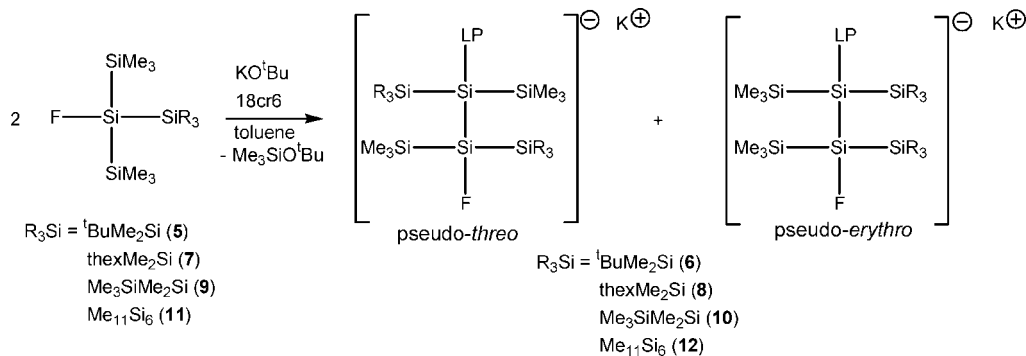
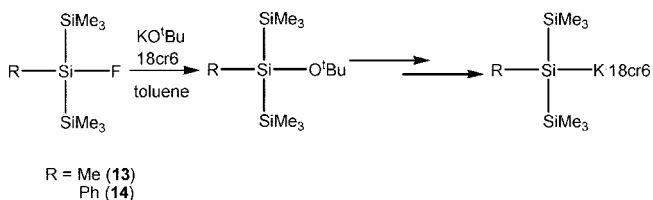


**Figure 4.** Formal adduct formation processes starting from disilene **4** by addition of KF or fluoride ion. The upper panel corresponds to the structural motif of **3a**, where the two observed coordination positions are on the same side of the formal disilene. The lower panel corresponds to the structural motif of **3b**, where the two observed coordination positions are on different sides of the formal disilene.

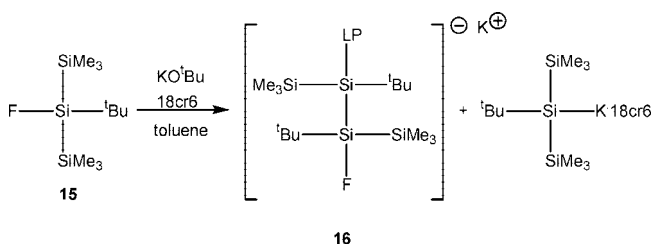
**Scheme 2.** Reactions of Oligosilylfluorides with KO<sup>t</sup>Bu Leading to Fluoride Disilene Adducts



**Scheme 3.** Reactions of **13** and **14** To Form the Respective Silyl Ethers and Subsequently the Silyl Anions

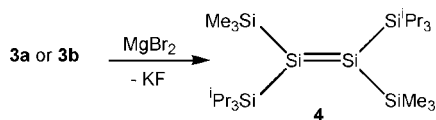


**Scheme 4.** Reaction of **15** To Form a Mixture of Disilene Adduct **16** and the Oligosilyl Anion



adducts by the direct reaction of a disilene with a suitable Lewis base, we reacted **4** with potassium and cesium fluoride in the presence of 18-crown-6. No adduct formation was observed. Attempts to react **4** with triethylamine and trimethylphosphine were also futile. Using a more powerful base such as potassium *tert*-butoxide led to the formation of the corresponding alkoxide adduct, which is related to the products obtained by self-condensation of alkoxy-substituted silylenoids.<sup>8,12</sup>

**NMR Spectroscopy.** The formation of the disilene adducts is easily followed by NMR spectroscopy. With <sup>29</sup>Si and especially <sup>19</sup>F, two nuclei that display favorable NMR properties, such as a broad range of shifts and, in the case of <sup>19</sup>F, very good sensitivity, are involved. <sup>19</sup>F chemical shifts were found to be the most useful for reaction monitoring. The trisilylated starting materials all exhibit resonances around -250 ppm, while the disilene adduct resonances are shifted downfield to values

**Scheme 5.** Reaction of **3a** or **3b** with Magnesium Bromide To Form Disilene **4**

between  $-195$  and  $-213$  ppm. In contrast, silylenoid resonances were found to be shifted upfield to values close to  $-280$  ppm (Table 1).

The  $J_{\text{Si-F}}$  coupling pattern allows for a very simple identification of the involved compounds. Some trends that depended on the classes of compounds involved were observed. All of the silyl fluoride starting materials display strong  $^1J_{\text{Si-F}}$  coupling, with coupling constants between 324 and 335 Hz. Upon formation of the silylenoid, a slight increase in the  $^1J_{\text{Si-F}}$  coupling constant was observed, from 324 Hz for **1** to 355 Hz for **2** [which compares well to the value of 356.5 Hz reported for  $(\text{tert-Bu}_3\text{Si})_2\text{Si}(\text{F})\text{Li}^{11}$ ] and from 335 Hz for **11** to 375 Hz for  $(\text{Me}_{11}\text{Si}_6)(\text{Me}_3\text{Si})\text{Si}(\text{F})\text{K}$ .

The values of  $^1J_{\text{Si-F}}$  and  $^2J_{\text{Si-F}}$  for the disilene fluoride adducts seem to indicate that **3a** and **3b** are not only different in the crystal but show also a distinctly different behavior in solution (Table 1). For the THF adduct **3b**, both the  $^1J_{\text{Si-F}}$  and  $^2J_{\text{Si-F}}$  coupling constants (292 and 90.5 Hz, respectively) are significantly different from all of the other observed values for the crown ether disilene adducts. For the latter, values for  $^1J_{\text{Si-F}}$  were found to be in the range 314–342 Hz, while the observed  $^2J_{\text{Si-F}}$  couplings were 45–79 Hz. On the basis of the results of the computational study (see below), the magnitudes of the  $^1J_{\text{Si-F}}$  coupling constants suggest that both **3a** and **3b** have the same conformation in solution (pseudo-*threo*). In addition, the  $^2J_{\text{Si-F}}$  coupling constants indicate that there is some interaction between potassium and the fluorine atom in solution for the case of **3b**. For **3a** and all of the other crown ether adducts, this interaction is either nonexistent or much weaker.

$^{29}\text{Si}$  NMR data are also useful for examining the electronic state of the molecules. The resonances found for the trisilylated silylfluorides are all in the 33.4–45.3 ppm range found for similar compounds (Table 1). The difference between the  $^{29}\text{Si}$  spectra of **3a** and **3b** is interesting. The crown ether adduct **3a** exhibits a resonance at 62.3 ppm for the silicon atom bearing the fluoride substituent, while the anionic silicon atom resonates at a rather typical  $-175$  ppm. In comparison with this, the corresponding signals for the THF adduct **3b** are both shifted downfield by  $\sim 10$  ppm. It is likely that these changes can also be associated with the different degree of interaction between potassium and fluoride in **3a** and **3b**. For compounds **6**, **8**, and **10**, two sets of resonances were found, which we attribute to the existence of diastereomeric mixtures. While we found that the resonances for the fluoride-substituted silicon atoms are close for the two diastereomers ( $\pm 5$  ppm), those for the negatively charged silicon atoms seem to be more sensitive to the steric environment, showing chemical shifts that differ by as much as 13 ppm.

**Crystal Structure Analyses.** Compounds **3a**, **3b**, **4**, and **11** could be subjected to crystal structure analyses (Table 2). The quality of the solution for **3a** was not very good. Nevertheless, the comparison of **3a** and **3b** offers some insight. The structure of **3a** (Figure 1), which crystallizes in the monoclinic space group  $C2/c$ , resembles the one obtained for the crown ether adduct of  $(\text{Me}_3\text{Si})_2\text{FSiSiK}(\text{SiMe}_3)_2$ .<sup>9</sup> The  $C_2$ -symmetric polysilane part adopts an eclipsed sawhorse conformation, and the

fluoride ion is distributed evenly over the two possible sites, suggesting that there is  $C_2$ -symmetric disorder of the molecule in the solid state. In addition, there was some disorder found in one of the triisopropylsilyl groups. The potassium atom, which exhibits equal interaction with the two fluorine atom sites, resides at a distance of 2.78 Å. Formally, the formation of the disilene adduct may be envisaged as a fluoride ion approaching the (*E*)-disilene, which causes both central silicon atoms to rehybridize to  $sp^3$  (Figure 4). Interestingly, at least in the solid state, the geometry of the acceptor silicon atom seems to be nearly the same as that of its now anionic neighbor. This feature allows for the mentioned disorder, as the two possible spatial arrangements have the same steric requirements with respect to the polysilane part. The length of the central Si–Si bond of **3a** is 2.321(3) Å, which is longer than the distance of 2.293(2) Å found for the crown ether adduct of  $(\text{Me}_3\text{Si})_2\text{FSiSiK}(\text{SiMe}_3)_2$ .<sup>9</sup> This may be ascribed to the increased steric bulk of the triisopropylsilyl groups. The large bond angle of  $125.12(8)^\circ$  for Si(1A)–Si(1)–Si(3) also supports this assumption. The Si–F bond [1.556(5) Å] is also longer than was found for  $(\text{Me}_3\text{Si})_2\text{FSiSiK}(\text{SiMe}_3)_2$ <sup>9</sup> but substantially shorter than the corresponding distance found in Wiberg's silene fluoride adduct (1.647 Å).<sup>5c</sup>

In contrast to **3a**, the structure of **3b** (Figure 2) presents itself as an ion pair. The potassium ion is coordinated by six THF molecules and thus separated from the fluoride adduct part. The polysilane moiety now exhibits a staggered sawhorse conformation, and the fluoride ion is distributed evenly over two possible sites on different sides of the formal disilene part. Again, the formation of the disilene adduct may be envisaged as a fluoride ion approaching the (*E*)-disilene (Figure 4). However, this time the fluoride approach effects the rehybridization of the negatively charged silicon in the opposite configuration. This gives rise to the formation of the other diastereomer. Again, the spatial environments of the anionic silicon atom and the fluoride-coordinated one are nearly identical. The length of the central Si–Si bond of **3b** [2.3285(13) Å] is nearly the same as that of **3a**. In contrast to this, the Si–F distance of 1.492(2) Å is substantially shorter than in **3a** but longer than in the crown ether adduct of  $(\text{Me}_3\text{Si})_2\text{FSiSiK}(\text{SiMe}_3)_2$ .<sup>9</sup>

The structure of disilene **4** (Figure 5) is very similar to what has been found for other fourfold-silyl-substituted disilenes.<sup>16</sup> The length of the Si–Si double bond is 2.1967(11) Å, which is well within the 2.17–2.26 Å range found for related compounds.<sup>16</sup>

The structure of the undecamethylcyclohexasilanyl-substituted bis(trimethylsilyl)silyl fluoride **11** (Figure 6) is also close to what could be expected. The Si–Si bond lengths are between 2.34 and 2.36 Å, and the respective bond angles are close the ideal tetrahedral angle. The rather long Si–F bond distance<sup>17</sup> of 1.6396(18) Å is almost identical to that of the only known structurally related example.<sup>18</sup> The cyclohexasilane part adopts a typical chair conformation with the bis(trimethylsilyl)fluorosilyl substituent in an equatorial position.

**Computational Analysis.** In the first part of the computational investigation, the feasibility of the formation of disilene fluoride adducts was studied. With the silylenoid  $(\text{H}_3\text{Si})_2\text{FSiLi}\cdot(\text{OMe})_3$  as a starting point, the process of formation of dimers was studied. Two stable dimeric structures were obtained (see Figure 7). These dimers are more stable than the corresponding monomers ( $\Delta G_{\text{stab}} = -23.0$  and  $-22.8$  kJ/mol at 298.15 K). Removal of one lithium fluoride unit from the dimers describes the feasibility of disilene fluoride adduct formation. Alterna-

**Table 1.**  $^{29}\text{Si}$  and  $^{19}\text{F}$  NMR Shifts (ppm) and Coupling Constants (Hz)

compound	$^{29}\text{Si}$ $\delta_{\text{Si-F}}$	$^1J_{\text{Si-F}}$	$^{29}\text{Si}$ $\delta_{\text{Si-K}}$	$^{19}\text{F}$ $\delta$
$(\text{Me}_3\text{Si})_3\text{SiF}$	34.0	327.4		-255.9
$(\text{Me}_3\text{Si})_2\text{FSiSiK}$ - $(\text{SiMe}_3)_2 \cdot 18\text{-crown-6}$	58.6	314.0	-169.3	-213.5
<b>1</b>	40.1	324.0		-250.5
<b>2</b>	85.8	355.1	85.8	-287.9
<b>3a</b>	62.3	342.1	-175.8	-201.0
<b>3b</b>	72.3	291.9	-162.1	-195.8
<b>5</b>	35.6	327.7		-252.6
<b>6</b>	63.6/61.6 <sup>a</sup>	317.9/321.8 <sup>a</sup>	-171.2/-162.0 <sup>a</sup>	-211.5/-207.2 <sup>a</sup>
<b>7</b>	33.4	326.5		-249.1
<b>8</b>	62.5/57.6 <sup>a</sup>	326.7/342.7 <sup>a</sup>	-179.7/-166.1 <sup>a</sup>	-213.7/-206.6 <sup>a</sup>
<b>9</b>	38.7	329.4		-250.2
<b>10</b>	61.2/61.1	345.8/340.7 <sup>a</sup>	-167.5/-167.7 <sup>a</sup>	-205.4/-204.0 <sup>a</sup>
<b>11</b>	45.3	335.0		-241.5
$(\text{Me}_{11}\text{Si}_6)$ - $(\text{Me}_3\text{Si})\text{Si}(\text{F})\text{K}$	—	375.0		-274.1
<b>12</b>	70.9	340.8	-179.8	-204.9
<b>13</b>	36.2	324.3		-209.7
<b>14</b>	26.9	327.2		-216.9
<b>15</b>	39.0	333.1		-213.9
<b>16</b>	65.2	324.6	-61.1	-187.6

<sup>a</sup> Mixture of diastereomers.**Table 2.** Crystallographic Data for Compounds **3a**, **3b**, **4**, and **11**

	<b>3a</b>	<b>3b</b>	<b>4</b>	<b>11</b>
empirical formula	$\text{KFO}_6\text{Si}_6\text{C}_{36}\text{H}_{84}$	$\text{KFO}_6\text{Si}_6\text{C}_{48}\text{H}_{108}$	$\text{Si}_6\text{C}_{24}\text{H}_{60}$	$\text{Si}_9\text{FC}_{17}\text{H}_{51}$
molecular weight	839.67	1007.98	517.26	527.39
temperature (K)	100(2)	100(2)	100(2)	100(2)
size (mm)	$0.50 \times 0.42 \times 0.34$	$0.48 \times 0.36 \times 0.30$	$0.45 \times 0.15 \times 0.15$	$0.34 \times 0.22 \times 0.22$
crystal system	monoclinic	triclinic	monoclinic	monoclinic
space group	$C2/c$	$P\bar{1}$	$C2/c$	$P2_1/c$
<i>a</i> (Å)	23.907(5)	10.700(2)	20.967(4)	10.041(2)
<i>b</i> (Å)	12.136(2)	11.556(2)	8.246(2)	16.881(3)
<i>c</i> (Å)	19.718(4)	12.860(3)	20.565(4)	20.115(4)
$\alpha$ (deg)	90	103.33(3)	90	90
$\beta$ (deg)	120.50(3)	93.43(3)	108.63(3)	100.84(3)
$\gamma$ (deg)	90	97.87(3)	90	90
<i>V</i> (Å <sup>3</sup> )	4929.3(2)	1525.8(5)	3369.2(2)	3348.7(2)
<i>Z</i>	4	1	4	4
$\rho_{\text{calc}}$ (g cm <sup>-3</sup> )	1.131	1.097	1.020	1.046
absorption coefficient (mm <sup>-1</sup> )	0.294	0.247	0.258	0.367
<i>F</i> (000)	1840	556	1152	1152
$\theta$ range	$1.95 < \theta < 24.00$	$1.63 < \theta < 26.37$	$2.05 < \theta < 26.32$	$1.59 < \theta < 26.38$
reflections collected/unique	15857/3874	11982/6106	12902/3422	19810/6655
completeness to $\theta$ (%)	100	97.8	99.8	97.1
data/restraints/parameters	3874/138/346	6106/0/295	3422/0/145	6655/0/261
goodness of fit on <i>F</i> <sup>2</sup>	1.06	1.04	1.26	1.02
final R1, wR2 [ <i>I</i> > 2 $\sigma$ ( <i>I</i> )]	0.094, 0.227	0.047, 0.129	0.047, 0.106	0.051, 0.128
R1, wR2 (all data)	0.107, 0.237	0.054, 0.135	0.049, 0.107	0.071, 0.139
largest diff. peak, hole (e/Å <sup>3</sup> )	0.94, -0.99	0.97, -0.45	0.56, -0.18	1.19, -0.28

tively, these compounds can be envisaged to form starting from the respective disilenes upon addition of lithium fluoride (the same way as shown in Figure 4). Calculating the interaction of the planar tetrasilyldisilene<sup>19</sup> with a separated fluoride anion as the simplest Lewis base model results in strong covalent bonding, forming fluorodisilanide. The presence of a counterion, such as Li, interacting with the fluoride ion diminishes the degree of this interaction. The crystal structures of **3a** and **3b** do not mirror this effect, since the Si–F distance in **3b** is only slightly smaller than that in **3a**, despite the fact that the potassium cation is completely separated. To model solvent effects, the cation was surrounded with three Me<sub>2</sub>O molecules, accounting for the THF molecules used in the synthesis. The interaction of tetrasilyldisilene with FLi•(OMe)<sub>3</sub> resulted in two possible stable adduct conformers. The more stable adduct **A**, features the stereochemical situation found in the crystal structure of

**3a**, while structure **B**, which is similar to the crystal structure of **3b**, is 10.7 kJ/mol less stable (see Figure 8). The energy gain upon adduct formation is  $\Delta G_{\text{stab}} = G_{\text{adduct}} - (G_{\text{FLi}(\text{OMe})_3} + G_{\text{disilene}}) = -91.6$  kJ/mol for adduct **A**. The interaction with the ion pair has dramatic structural consequences for the disilene. In a way similar to that for the interactions between silenes and lithium fluoride described previously,<sup>5a</sup> the Si=Si bond of tetrasilyldisilene elongates from 2.162 to 2.324 Å in **A** and 2.297 Å in **B**. The silicon bond angle sums decrease from 360° to 347.9°/300.7° in **A** and 331.6°/299.6° in **B**, indicating a strong degree of pyramidalization. As the Li–F bond weakens, the lithium cation can move from fluorine to the negatively charged Si2 atom, forming the lithium fluorodisilanide **C**, which is 4.2 kJ/mol more stable than **A** (see Figure 8).

As a result of the adduct formation, negative charge is transferred to the tricoordinated silicon atom (Si2). The calcu-

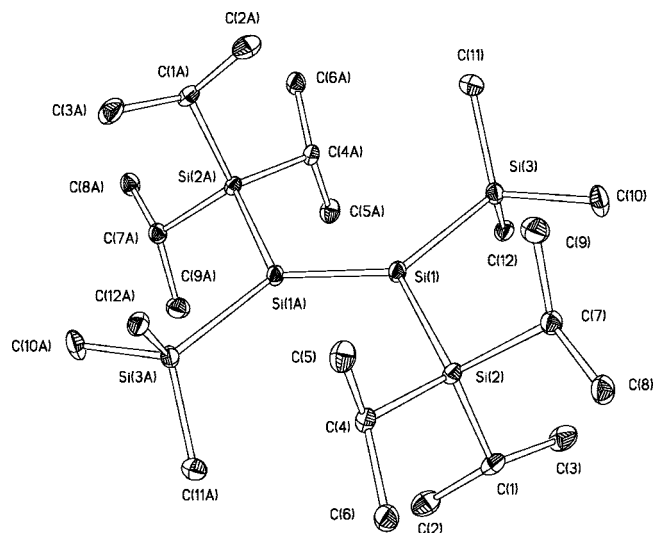


**Figure 5.** Molecular structure and numbering of **4**. Selected bond lengths (Å) and bond angles (deg): Si(1)–Si(1A), 2.1967(11); Si(1)–Si(2), 2.3710(10); Si(1)–Si(3), 2.3746(9); Si(2)–C(1), 1.902(2); Si(1A)–Si(1)–Si(2), 122.98(4); Si(1A)–Si(1)–Si(3), 120.79(4); Si(2)–Si(1)–Si(3), 114.65(3).

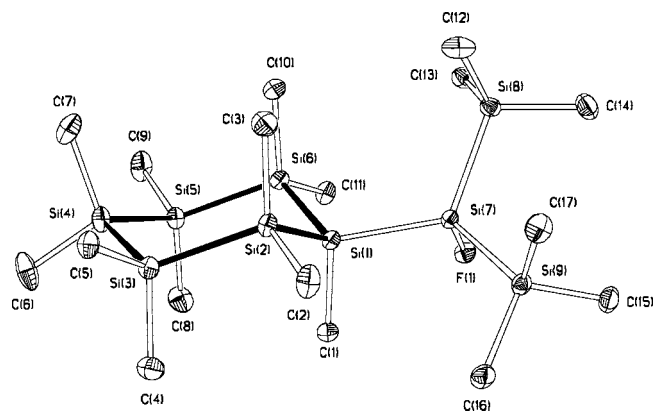


**Figure 6.** Molecular structure and numbering of **11**. Selected bond lengths (Å) and bond angles (deg): Si(1)–C(1), 1.909(3); Si(1)–Si(2), 2.3396(12); Si(1)–Si(6), 2.3456(12); Si(1)–Si(7), 2.3567(11); Si(7)–F(1), 1.6396(18); Si(7)–Si(8), 2.3557(11); Si(2)–Si(1)–Si(6), 109.07(5); Si(2)–Si(1)–Si(7), 18.44(4); Si(6)–Si(1)–Si(7), 110.51(5); Si(1)–Si(2)–Si(3), 110.29(4); Si(4)–Si(3)–Si(2), 113.92(5); Si(3)–Si(4)–Si(5), 113.01(5); Si(6)–Si(5)–Si(4), 113.69(4); Si(5)–Si(6)–Si(1), 109.93(4); F(1)–Si(7)–Si(8), 104.35(7); F(1)–Si(7)–Si(1), 100.84(7); F(1)–Si(7)–Si(9), 105.28(7); Si(8)–Si(7)–Si(9), 110.35(4); Si(1)–Si(7)–Si(9), 113.82(5).

lated  $^{29}\text{Si}$  NMR chemical shifts mirror this nicely. While  $\delta_{^{29}\text{Si}1}$  is 88.7 and 69.8 ppm in **A** and **B**, respectively, the corresponding  $\delta_{^{29}\text{Si}2}$  values are strongly downfield-shifted to  $-168.4$  and  $-159.6$  ppm, which fall into the typical range of chemical shifts for trisilylated silyl anions.<sup>15</sup>

It was hoped that the calculation of F–Si coupling constants would serve as a means of assessing the conformational situation in solution. Different lithium disilanides (Figure 9) and two disilanide ions (Figure 10) were studied.

It was found that the calculated F–Si coupling constants differ considerably for the investigated conformers. Depending on the conformation of the disilanide unit, the  $^1J_{\text{F-Si}}$  value was found to be close to  $-486$  Hz for the **B**-type geometry and to  $-300$  Hz for the **A**-type geometry. The  $^2J_{\text{F-Si}}$  coupling to the negatively charged silicon atom is rather sensitive to the presence of a counterion. Removal of the lithium counterion causes those  $^2J_{\text{F-Si}}$  couplings to decrease to 73.3 and 33.9 Hz (Figure 10) from the values of close to 130 Hz for the ion pairs (Figure 9). The calculated coupling constants were compared to the experimentally determined solution NMR data for **3a** and **3b** (Figure 10). The very poor agreement between the calculated data for the geometry in the solid state suggests that both the conformation and coordination are different in solution for **3a** and **3b**. When the calculated numbers are compared to the experimentally determined data, the following seems to be likely: The crown ether adduct **3a** possesses the same geometry as in the solid state, but the interaction between the fluorine atom and the potassium counterions is strongly diminished. The conformation of **3b** in solution seems to be the same that of **3a**, but in contrast to the solid-state case, some interaction of fluorine and potassium takes place (diminishing the value of  $^1J_{\text{Si-F}}$ ). Considering the fact that the studies were carried out in  $\text{C}_6\text{D}_6$  solution, it seems reasonable to imagine that some THF dissociates from the potassium cation. Thus, coordination to the fluoride becomes possible. In contrast to this, the crown ether of **3a** can be expected to coordinate strongly at all times.

## Conclusion

We recently reported that the reaction of  $(\text{Me}_3\text{Si})_3\text{SiF}$  with potassium *tert*-butoxide leads to the formation of the  $\beta$ -fluorodisilanyl anion  $(\text{Me}_3\text{Si})_2\text{FSiSiK}(\text{SiMe}_3)_2$ .<sup>9</sup> Another description of this compound might be that of a disilene fluoride adduct. Such adducts have been the subject of speculation by Wiberg but were thought to form only with polarized  $\text{Si}=\text{E}$  systems. In the present work, we have extended our studies of the formation of disilene fluoride adducts. It was shown that their formation clearly proceeds via the self-condensation of fluorosilylenoids. Depending on the steric properties of the silyl groups attached to the fluorosilylenoid, the condensation selectively yields either one or, in case of comparable sizes of the silyl groups, mixtures of the two possible diastereomers. It was shown that upon treatment with magnesium bromide,  $(\text{Me}_3\text{Si})(^i\text{Pr}_3\text{Si})\text{FSiSiK}(\text{SiMe}_3)(\text{Si}^i\text{Pr}_3)$  yields the (*E*)-disilene, which was found to be stable. Attempts were made to extend the scope of the disilene adduct formation reaction by exchanging one silyl group in the starting material for a methyl, phenyl, or *tert*-butyl group. However, a different course of reaction was observed for the methyl and phenyl cases, where the diminished steric demand of the organic group facilitates attack of the alkoxide at the central silicon atom, thus leading to the formation of silyl-*tert*-butyl ethers. The *tert*-butyl-substituted example led to the formation of the expected disilene adduct, which, however, was accompanied by the formation of *tert*-butyl-bis(trimethylsilyl)silylpotassium.

(16) (a) Kira, M.; Maruyama, T.; Kabuto, C.; Ebata, K.; Sakurai, H. *Angew. Chem.* **1994**, *106*, 1575–1577; Kira, M.; Maruyama, T.; Kabuto, C.; Ebata, K.; Sakurai, H. *Angew. Chem., Int. Ed. Engl.* **1994**, *33*, 1489–1491. (b) Kira, M.; Ohya, S.; Iwamoto, T.; Ichinohe, M.; Kabuto, C. *Organometallics* **2000**, *19*, 1817–1819. (c) Iwamoto, T.; Okita, J.; Kabuto, C.; Kira, M. *J. Organomet. Chem.* **2003**, *686*, 105–111. (d) Sekiguchi, A.; Inoue, S.; Ichinohe, M.; Arai, Y. *J. Am. Chem. Soc.* **2004**, *126*, 9626–9629.

(17) Kaftory, M.; Kapon, M.; Botoshansky, M. In *The Chemistry of Organic Silicon Compounds*; Rappoport, Z., Apeloig, Y., Eds.; Wiley: New York, 1998; Vol. 2, Chapter 5.

(18) Chichian, S.; Kempe, R.; Krempner, C. *J. Organomet. Chem.* **2000**, *613*, 208–219.

(19) (a) Karni, M.; Apeloig, Y. *J. Am. Chem. Soc.* **1990**, *112*, 8589–8590. (b) Liang, C.; Allen, L. C. *J. Am. Chem. Soc.* **1990**, *112*, 1039–1041.



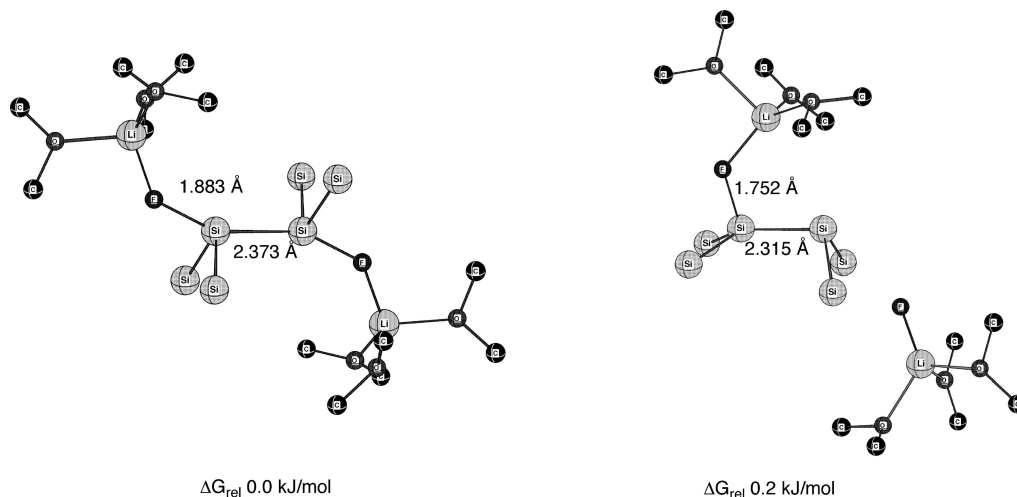


Figure 7. Structures of dimers of the silylenoid  $(\text{H}_3\text{Si})_2\text{FSiLi}\cdot(\text{OMe})_3$  obtained from calculations at the mPW1PW91/6-31+\* level.

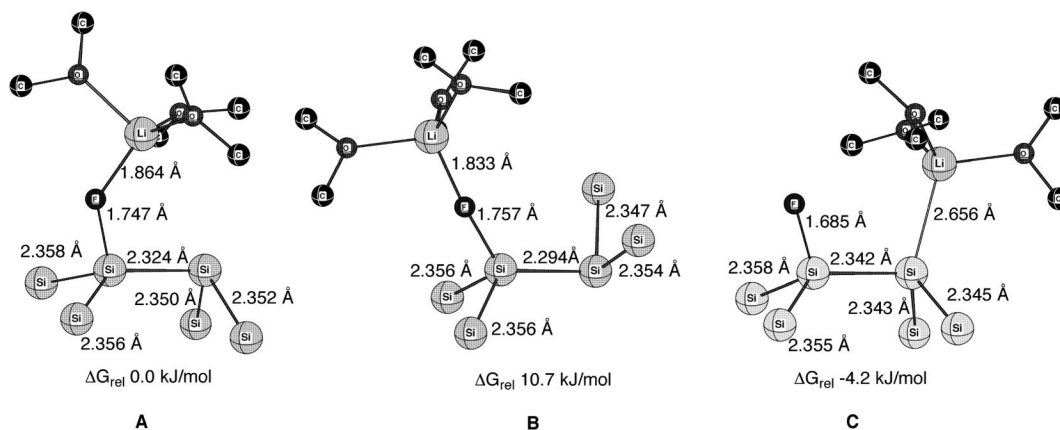


Figure 8. mPW1PW91/6-31+G\*-optimized structures of tetrasilyldisilene interacting with  $\text{FLi}\cdot(\text{OMe})_3$ .

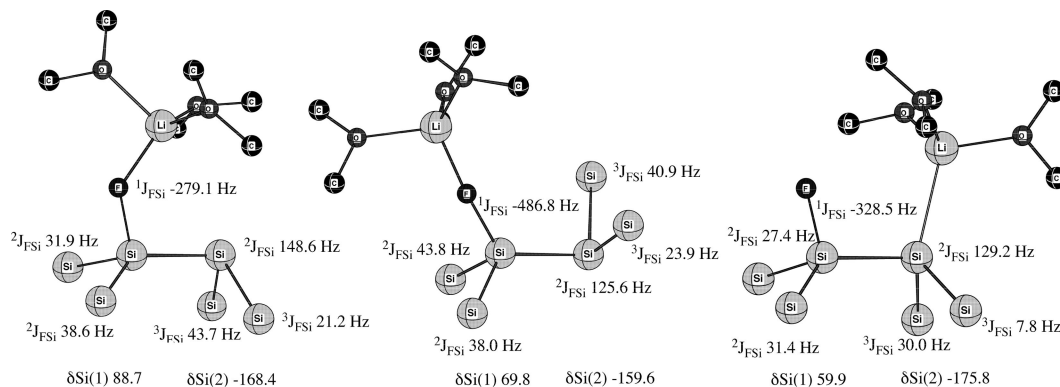


Figure 9. BHAndHLYP/IGLO-III-calculated coupling constants and PW91/IGLO-II-calculated chemical shifts for the lithium disilanide conformers.

In a way similar to that previously pointed out for silene adducts, disilene fluoride adducts can also be considered as instant precursors of disilenes which might not be stable under ambient conditions. By addition of magnesium bromide, the disilenes can then be liberated in the presence of a suitable trapping reagent.

## Experimental Section

**General Remarks.** All of the reactions involving air-sensitive compounds were carried out under an atmosphere of dry nitrogen

or argon using either Schlenk techniques or a glovebox. Solvents were dried using a column solvent purification system.<sup>20</sup> Potassium *tert*-butanolate was purchased from Merck. All of the other chemicals were bought from various suppliers and were used without further purification.  $^1\text{H}$  (300 MHz),  $^{13}\text{C}$  (75.4 MHz),  $^{19}\text{F}$  (282.2 MHz), and  $^{29}\text{Si}$  (59.3 MHz) NMR spectra were recorded on a Varian INOVA 300 spectrometer. Samples for  $^{29}\text{Si}$  spectra were either dissolved in a deuterated solvent or

(20) Pangborn, A. B.; Giardello, M. A.; Grubbs, R. H.; Rosen, R. K.; Timmers, F. J. *Organometallics* **1996**, *15*, 1518–1520.

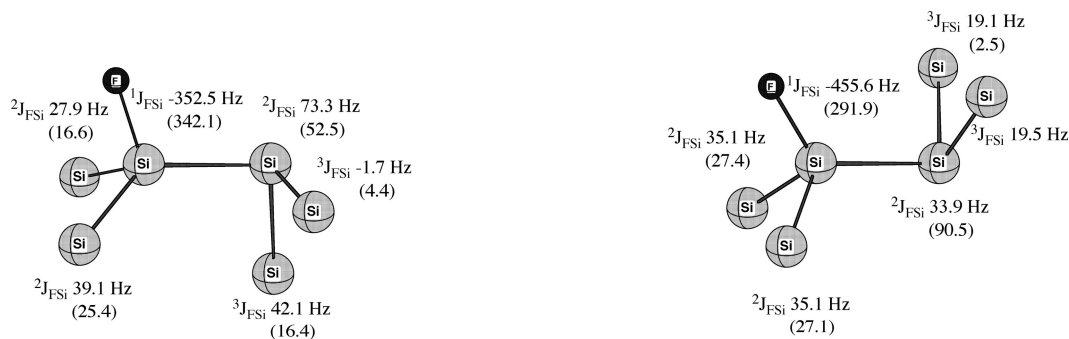


**Figure 10.** Calculated coupling constants for the separated disilane units (geometries taken from the crystal structures of **3a** and **3b**). The experimentally determined coupling constants for **3a** and **3b** in  $C_6D_6$  solution are given in parentheses.

measured with a  $D_2O$  capillary in order to provide an external lock-frequency signal. To compensate for the low isotopic abundance of  $^{29}Si$ , the INEPT pulse sequence was used for the amplification of the signal.<sup>21</sup> Elemental analyses were carried out using a Heraeus Vario Elementar analyzer.

**Computational Details.** Geometries were optimized at the mPW1PW91/6-31+G\* level of theory using Gaussian03.<sup>22</sup> The nature of the stationary points was verified by analytical frequency calculations. Adduct and dimer stabilities were obtained by subtracting the sum of the fragment energies from the adduct/dimer energy [i.e.,  $\Delta G_{stab} = G_{AB} - (G_A + G_B)$ ]. For the nuclear spin–spin coupling constants, the half-and-half hybrid functional BHandHLYP as implemented in Gaussian03 was applied together with IGLO-III basis sets.

Magnetic shieldings were computed using the SOS-DFPT IGLO Perdew–Wang91/IGLO-II method with the deMon/NMR program.<sup>23</sup> For the  $^{29}Si$  NMR chemical shifts, tetramethylsilane was used as a reference, with  $\sigma_{29Si}^0 = 364.6$  ppm calculated at the same level of theory.

**X-ray Structure Determination.** For X-ray structure analyses, the crystals were mounted onto the tips of glass fibers, and data collection was performed with a Bruker-AXS SMART APEX CCD diffractometer using graphite-monochromatized Mo  $K\alpha$  radiation ( $\lambda = 0.71073$  Å). The data were reduced to  $F_o^2$  and corrected for absorption effects with SAINT<sup>24</sup> and SADABS,<sup>25</sup> respectively. The structures were solved by direct methods and refined by full-matrix least-squares methods (SHELXL97).<sup>26</sup> Unless noted otherwise, all of the non-hydrogen atoms were refined with anisotropic displacement parameters. All of the hydrogen atoms were located in calculated positions corresponding to standard bond lengths and angles. All of the structures were drawn with thermal ellipsoids at the 30% probability level and all of the hydrogen atoms omitted for clarity. Crystallographic data (excluding structure factors) for the structures of compounds **3a**, **3b**, **4**, and **11** reported in this paper have been deposited with the Cambridge Crystallographic Data Centre (CCDC) as supplementary publication nos. CCDC-661270

(**3a**), 661272 (**3b**), 661271 (**4**), and 694224 (**11**). Copies of the data can be obtained free of charge at <http://www.ccdc.cam.ac.uk/products/csd/request/>.

**Syntheses.** Triisopropylsilyltris(trimethylsilyl)silane,<sup>27</sup> *tert*-butyldimethylsilyltris(trimethylsilyl)silane,<sup>27,28</sup> 1,1,1-tris(trimethylsilyl)-2,2-dimethyl-2-hexyldisilane,<sup>27</sup> chloromethylbis(trimethylsilyl)silane,<sup>29</sup> chlorobis(trimethylsilyl)phenylsilane,<sup>30</sup> difluorobis(trimethylsilyl)silane,<sup>29</sup> undecamethylcyclohexanilylbis(trimethylsilyl)silane,<sup>31</sup> tris(trimethylsilyl)pentamethyldisilanyl silane,<sup>28</sup>  $[Ph_3SnF_2][NBu_4]$ ,<sup>32</sup> and  $MgBr_2 \cdot Et_2O$ <sup>33</sup> were prepared according to published procedures.

**2-Fluoro-1,2-bis(trimethylsilyl)-1,2-bis(triisopropylsilyl)disilanylpotassium·18-crown-6 (3a).** Compound **1** (80 mg, 0.23 mmol) was dissolved in toluene (3 mL), and 18-crown-6 (60 mg, 1 equiv) and potassium *tert*-butanolate (26 mg, 1 equiv) were added. The solution immediately turned orange. After 30 min, the intermediate formation of **2** could be observed. Stirring was continued for 2 days at room temperature (r.t.) until complete conversion was achieved (as determined by  $^{29}Si$  NMR spectroscopy). The precipitate was removed by centrifugation and the solvent in vacuum. The residue was dissolved again in toluene and cooled to  $-70$  °C. At this temperature, an orange crystalline product (69 mg, 72%) was obtained.  $^{29}Si$  NMR ( $C_6D_6$ )  $\delta$  (ppm): 62.3 (d,  $J_{Si-F} = 342.1$  Hz,  $Si-F$ ); 22.8 (d,  $J_{Si-F} = 16.6$  Hz,  $^iPr_3Si-Si-F$ );  $-4.7$  (d,  $J_{Si-F} = 16.4$  Hz,  $^iPr_3Si-Si-K$ );  $-8.2$  (d,  $J_{Si-F} = 4.4$  Hz,  $Me_3Si-Si-K$ );  $-17.3$  (d,  $J_{Si-F} = 25.4$  Hz,  $Me_3Si-Si-F$ );  $-175.8$  (d,  $J_{Si-F} = 52.5$  Hz,  $Si-K$ ).  $^1H$  ( $C_6D_6$ )  $\delta$  (ppm): 3.32 (s, 24H,  $CH_2O$ ); 1.61 (m, 6H,  $(CH_3)_2-CH-$ ); 1.57 (m, 36H,  $(CH_3)_2-CH$ ); 0.73 (s, 9H,  $-Si(CH_3)_3$ ); 0.66 (s, 9H,  $-Si(CH_3)_3$ ).  $^{13}C$  NMR ( $C_6D_6$ )  $\delta$  (ppm): 70.3; 22.0; 21.6; 16.3; 14.9; 9.3; 2.9.  $^{19}F$  NMR ( $C_6D_6$ )  $\delta$  (ppm):  $-200.96$  ( $J_{Si-F} = 343.3$  Hz).

**Fluorotrimethylsilyltrisopropylsilylpotassium·18-crown-6 (2).**  $^{29}Si$  NMR ( $C_6D_6$ )  $\delta$  (ppm): 85.8 (d,  $J_{Si-F} = 355.1$  Hz,  $Si-F$ ); 5.4 (d,  $J_{Si-F} = 10.0$  Hz,  $^iPr_3Si$ );  $-13.8$  (d,  $J_{Si-F} = 15.4$  Hz,  $Me_3Si$ ).  $^1H$  ( $C_6D_6$ )  $\delta$  (ppm): 3.27 (s, 24H,  $CH_2O$ ); 1.51 (m, 3H,  $-CH(CH_3)_2$ ); 1.44 (d, 18H,  $J_{H-H} = 6.4$  Hz,  $-CH(CH_3)_2$ ); 0.56 (s, 9H,  $Si(CH_3)_3$ ).  $^{13}C$  NMR ( $C_6D_6$ )  $\delta$  (ppm): 70.1 ( $-OCH_2-$ ); 21.5 (d,  $J_{C-F} = 6.2$  Hz); 15.4 (d,  $J_{C-F} = 1.7$  Hz); 3.9 (d,  $J_{C-F} = 2.8$  Hz).  $^{19}F$  NMR ( $C_6D_6$ )  $\delta$  (ppm):  $-287.9$  ( $J_{Si-F} = 356.3$  Hz).

- (21) (a) Morris, G. A.; Freeman, R. *J. Am. Chem. Soc.* **1979**, *101*, 760–762. (b) Helmer, B. J.; West, R. *Organometallics* **1982**, *1*, 877–879.  
 (22) Frisch, M. J.; et al. *Gaussian 03*, revision C.02; Gaussian, Inc.: Wallingford, CT, 2004.  
 (23) (a) Salahub, D. R.; Fournier, R.; Mlynarski, P.; Papai, I.; St-Amant, A.; Ushio, J. In *Density Functional Methods in Chemistry*; Springer-Verlag: New York, 1991. (b) Malkin, V. G.; Malkina, O. L.; Eriksson, L. A.; Salahub, D. R. In *Theoretical and Computational Chemistry*; Elsevier: Amsterdam, 1995; Vol. 2, p. 273. (c) Kutzelnigg, W.; Fleischer, U.; Schindler, M. In *NMR Basic Principles and Progress*; Springer-Verlag: New York, 1991; Vol. 23, p. 167.  
 (24) *SAINTPUS Software Reference Manual*, version 6.45; Bruker-AXS: Madison, WI, 1997–2003.  
 (25) (a) Blessing, R. H. *Acta Crystallogr.* **1995**, *A51*, 33–38. (b) *SADABS*, version 2.1; Bruker-AXS: Madison, WI, 1998.  
 (26) Sheldrick, G. M. *Acta Crystallogr.* **2008**, *A64*, 112–122.  
 (27) Kayser, C.; Fischer, R.; Baumgartner, J.; Marschner, C. *Organometallics* **2002**, *21*, 1023–1030.

- (28) Apeloig, Y.; Yuzefovich, M.; Bendikov, M.; Bravo-Zhivotovskii, D.; Klinkhammer, K. *Organometallics* **1997**, *16*, 1265–1269.  
 (29) Schenzel, K.; Hassler, K. In *Organosilicon Chemistry II: From Molecules to Materials*; Auner, N., Weiss, J., Eds.; Verlag Chemie: Weinheim, Germany, 1996; pp 95–100.  
 (30) Baumeister, U.; Schenzel, K.; Zink, R.; Hassler, K. *J. Organomet. Chem.* **1997**, *543*, 117–124.  
 (31) Fischer, R.; Konopa, T.; Ullly, S.; Baumgartner, J.; Marschner, C. *J. Organomet. Chem.* **2003**, *685*, 79–92.  
 (32) (a) Gingras, M. *Tetrahedron Lett.* **1991**, *32*, 7381–7384. (b) Hummeltenberg, R.; Jurkschat, K.; Uhlrig, F. *Phosphorus, Sulfur Silicon Relat. Elem.* **1997**, *123*, 255–261.  
 (33) Nützel, K. In *Houben-Weyl, Methoden der Organischen Chemie*; Müller, E., Ed.; Georg Thieme Verlag: Stuttgart, Germany, 1973; Vol. 13/2a, p 76.

**2-Fluoro-1,2-bis(trimethylsilyl)-1,2-bis(triisopropylsilyl)disilanyl-potassium·6THF (3b).** To a solution of **1** (680 mg, 1.94 mmol) in THF (6 mL), potassium *tert*-butanolate (217 mg, 1 equiv) was added. The solution immediately turned red and was stirred for 3 h at r.t. until the reaction was complete (as determined by  $^{29}\text{Si}$  NMR). The solvent was removed in vacuo and the residue treated with pentane. The remaining precipitate was removed by centrifugation, and the solution was cooled to  $-70^\circ$ . At this temperature, a red crystalline product (507 mg, 52%) was obtained, which turned into an oil at r.t.  $^{29}\text{Si}$  NMR ( $\text{C}_6\text{D}_6$ )  $\delta$  (ppm): 72.3 (d,  $J_{\text{Si-F}} = 291.9$  Hz, Si-F); 22.4 (d,  $J_{\text{Si-F}} = 27.4$  Hz,  $^i\text{Pr}_3\text{Si-Si-F}$ ); -4.7 ( $^i\text{Pr}_3\text{Si-Si-K}$ ); -9.9 (d,  $J_{\text{Si-F}} = 2.5$  Hz,  $\text{Me}_3\text{Si-Si-K}$ ); -17.6 (d,  $J_{\text{Si-F}} = 27.1$  Hz,  $\text{Me}_3\text{Si-Si-F}$ ); -162.1 (d,  $J_{\text{Si-F}} = 90.5$  Hz, Si-K).  $^1\text{H}$  ( $\text{C}_6\text{D}_6$ )  $\delta$  (ppm): 3.42 (m, 4H, THF); 1.60 (m, 6H,  $(\text{CH}_3)_2\text{-CH-}$ ); 1.40 (m, 36H,  $2 \times (\text{CH}_3)_2\text{-CH-}$ ); 1.25 (m, 4H, THF); 0.51 (s, 9H,  $-\text{Si}(\text{CH}_3)_3$ ); 0.47 (s, 9H,  $-\text{Si}(\text{CH}_3)_3$ ).  $^{13}\text{C}$  NMR ( $\text{C}_6\text{D}_6$ )  $\delta$  (ppm): 67.7 (THF); 25.5 (THF); 21.4 (d,  $J_{\text{C-F}} = 5.0$  Hz,  $(\text{CH}_3)_2\text{-CH-}$ ); 21.1 (d,  $J_{\text{C-F}} = 9.2$  Hz,  $(\text{CH}_3)_2\text{-CH-}$ ); 15.7 (d,  $J_{\text{C-F}} = 1.5$  Hz,  $\text{CH}_3\text{-Si-Si-F}$ ); 14.7 ( $-\text{CH-}$ ); 8.2 ( $\text{Si}(\text{CH}_3)_3$ ); 2.1 ( $\text{Si}(\text{CH}_3)_3$ ).  $^{19}\text{F}$  NMR ( $\text{C}_6\text{D}_6$ )  $\delta$  (ppm): -195.8 ( $J_{\text{Si-F}} = 289$  Hz).

**(E)-1,2-Bis(trimethylsilyl)-1,2-bis(triisopropylsilyl)disilene (4).** To a solution of **3b** (200 mg, 0.33 mmol) in THF (2 mL),  $\text{MgBr}_2 \cdot \text{Et}_2\text{O}$  (88 mg, 1.05 equiv) was added. The reaction was complete after 30 min of stirring at r.t. (as determined by  $^{29}\text{Si}$  NMR), and the precipitate was removed by centrifugation. The solvent was removed and the residue treated with pentane. The remaining precipitate was removed by centrifugation, and the solution was cooled to  $-70^\circ$ . At this temperature, disilene **4** (103 mg, 61%) was obtained as an orange crystalline product.  $^{29}\text{Si}$  NMR ( $\text{C}_6\text{D}_6$ )  $\delta$  (ppm): 147.1; 18.9; -8.7.  $^1\text{H}$  ( $\text{C}_6\text{D}_6$ )  $\delta$  (ppm): 1.44 (m, 6H); 1.25 (d,  $J = 7.2$  Hz, 36H); 0.49 (s, 18H).  $^{13}\text{C}$  NMR ( $\text{C}_6\text{D}_6$ )  $\delta$  (ppm): 20.8; 15.3; 4.6. Anal. Calcd for  $\text{C}_{24}\text{H}_{60}\text{Si}_6$  (517.25): C, 55.73; H, 11.69. Found: C, 53.86; H, 11.60.

**2-Fluoro-1,2-bis(*tert*-butyldimethylsilyl)-1,2-bis(trimethylsilyl)disilanylpotassium·18-crown-6 (6).** The reaction was carried out in a manner analogous to that described above for the preparation of **3a**, using **5** (118 mg, 0.38 mmol),  $\text{KO}^t\text{Bu}$  (43 mg, 1 equiv), and 18-crown-6 (101 mg, 1 equiv). The reaction was complete after 3 h. Compound **6** was obtained as yellow crystals (119 mg, 41%) as a mixture of two isomers in a ratio of 3:1.

Data for *major-6*:  $^{29}\text{Si}$  NMR ( $\text{C}_6\text{D}_6$ )  $\delta$  (ppm): 63.6 (d,  $J_{\text{Si-F}} = 317.9$  Hz); 7.5 (d,  $J = 28.5$  Hz); -6.4 (d,  $J = 6.7$  Hz); -7.2 (d); -17.2 (d,  $J = 23.0$  Hz); -171.2 (d,  $J = 73.4$  Hz).  $^{19}\text{F}$  NMR ( $\text{C}_6\text{D}_6$ )  $\delta$  (ppm): -211.5 ( $J_{\text{Si-F}} = 318.9$  Hz;  $J_{\text{Si-F}} = 74.5$  Hz).

Data for *minor-6*:  $^{29}\text{Si}$  NMR ( $\text{C}_6\text{D}_6$ )  $\delta$  (ppm): 61.6 (d,  $J_{\text{Si-F}} = 321.8$  Hz); 7.5 (d,  $J = 28.5$  Hz); -6.9 (d); -7.0 (d); -17.3 (d,  $J = 23.5$  Hz); -162.0 (d,  $J = 76.6$  Hz).  $^{19}\text{F}$  NMR ( $\text{C}_6\text{D}_6$ )  $\delta$  (ppm): -207.2 ( $J_{\text{Si(1)-F}} = 322.4$  Hz;  $J_{\text{Si-F}} = 77.8$  Hz).

Data for **6** (mixture of isomers):  $^1\text{H}$  NMR ( $\text{C}_6\text{D}_6$ )  $\delta$  (ppm): 3.39(s); 1.40 (s); 1.35 (s); 1.32 (s); 1.11 (s); 0.73 (s); 0.71 (s); 0.68 (s); 0.66 (s); 0.61 (s); 0.60 (s); 0.48 (s); 0.44 (s).  $^{13}\text{C}$  NMR ( $\text{C}_6\text{D}_6$ )  $\delta$  (ppm): 70.7; 34.3; 32.3; 30.1; 29.0; 28.9; 22.6; 15.5; 14.1; 8.4; 8.1; 3.2; 3.0; 2.0; 1.8; -1.1; -2.5.

**2-Fluoro-1,2-bis(trimethylsilyl)-1,2-bis(dimethylhexylsilyl)disilanylpotassium·18-crown-6 (8).** The reaction was carried out in a manner analogous to that described above for the preparation of **3a**, using **7** (300 mg, 0.89 mmol),  $\text{KO}^t\text{Bu}$  (100 mg, 1 equiv), and 18-crown-6 (235 mg, 1 equiv). The reaction was complete after 3 h. Compound **8** was obtained as an orange oil (228 mg, 63%) as a mixture of two isomers in a ratio of 6:1.

Data for *major-8*:  $^{29}\text{Si}$  NMR ( $\text{C}_6\text{D}_6$ )  $\delta$  (ppm): 62.5 (d,  $J_{\text{Si-F}} = 326.7$  Hz); 9.7 (d,  $J_{\text{Si-F}} = 19.8$  Hz); -6.7 (d,  $J_{\text{Si-F}} = 23.5$  Hz); -6.5 (d,  $J_{\text{Si-F}} = 0.8$  Hz); -18.0 (d,  $J_{\text{Si-F}} = 24.0$  Hz); -179.7 (d,  $J_{\text{Si-F}} = 45.2$  Hz).  $^{19}\text{F}$  NMR ( $\text{C}_6\text{D}_6$ )  $\delta$  (ppm): -213.7 ( $J_{\text{Si-F}} = 326.8$  Hz;  $^2J_{\text{Si-F}} = 44.5$  Hz).

Data for *minor-8*:  $^{29}\text{Si}$  NMR ( $\text{C}_6\text{D}_6$ )  $\delta$  (ppm): 57.6 (d,  $J_{\text{Si-F}} = 342.7$  Hz); 6.5 (d,  $J_{\text{Si-F}} = 11.4$  Hz); -17.8 (d,  $J_{\text{Si-F}} = 26.8$  Hz);

-166.1 (d,  $J_{\text{Si-F}} = 57.2$  Hz).  $^{19}\text{F}$  NMR ( $\text{C}_6\text{D}_6$ )  $\delta$  (ppm): -206.6 ( $J_{\text{Si-F}} = 343.2$  Hz;  $^2J_{\text{Si-F}} = 56.0$  Hz,  $^3J_{\text{Si-F}} = 23.1$  Hz).

Data for **8** (mixture of isomers):  $^1\text{H}$  NMR ( $\text{C}_6\text{D}_6$ )  $\delta$  (ppm): 3.36(s); 1.33–1.15 (m); 0.91–0.84 (m); 0.69–0.61 (m,  $\text{SiMe}_3$ ); 0.13–0.07 (m).

**2-Fluoro-1,2-bis(trimethylsilyl)-1,2-bis(pentamethyldisilanyl)disilanylpotassium·18-crown-6 (10).** The reaction was carried out in a manner analogous to that described above for the preparation of **3a**, using **9** (185 mg, 0.57 mmol),  $\text{KO}^t\text{Bu}$  (64 mg, 1 equiv), and 18-crown-6 (151 mg, 1 equiv). After 1 h, complete conversion was observed. Compound **10** was obtained as a yellow oil (151 mg, 68%) as a mixture of two isomers in a ratio of 1:1. Cooling a pentane solution of **10** to  $-70^\circ\text{C}$  resulted in the precipitation of very fine, yellow, needle-shaped crystals. Data for **10** (mixture of isomers):  $^{29}\text{Si}$  NMR ( $\text{C}_6\text{D}_6$ )  $\delta$  (ppm): 61.2 (d,  $J_{\text{Si(1)-F}} = 345.8$  Hz); 61.1 ( $J_{\text{Si(1)-F}} = 340.7$  Hz); -6.4 (d,  $J = 14.6$  Hz); -6.5 (d,  $J = 12.0$  Hz);  $2 \times -15.0$  (d,  $J = 1.6$  Hz);  $2 \times -16.4$  (d,  $J = 2.9$  Hz); -17.5 (d,  $J = 25.5$  Hz); -17.6 (d,  $J = 27.6$  Hz); -33.8 (d,  $J = 3.4$  Hz); -34.6 (d,  $J = 16.7$  Hz); -43.5 (d,  $J = 32.6$  Hz); -43.6 (d,  $J = 32.2$  Hz); -167.5 (d,  $J_{\text{Si(2)-F}} = 60.7$  Hz); -167.7 (d,  $J_{\text{Si(2)-F}} = 58.1$  Hz).  $^1\text{H}$  NMR ( $\text{C}_6\text{D}_6$ )  $\delta$  (ppm): 3.36 (s, 48 H,  $-\text{OCH}_2-$ ); 0.65 (s, 9H); 0.64 (s, 9H); 0.61 (s); 0.55 (s); 0.54 (s); 0.47 (s); 0.42 (s); 0.40 (s).  $^{13}\text{C}$  NMR ( $\text{C}_6\text{D}_6$ )  $\delta$  (ppm): 70.4 ( $-\text{OCH}_2-$ ); 8.3; 8.1; 4.2; 4.0; 1.8; 1.7; 0.1; 0.0; -0.1; -1.5; -2.6 (d); -2.7 (d).  $^{19}\text{F}$  NMR ( $\text{C}_6\text{D}_6$ )  $\delta$  (ppm): -204.0 ( $J_{\text{Si(1)-F}} = 345.8$  Hz,  $J_{\text{Si(2)-F}} = 57.9$  Hz;  $J = 31.5$  Hz;  $J = 25.2$  Hz,  $J = 14.5$  Hz); -205.4 ( $J_{\text{Si(1)-F}} = 340.4$  Hz,  $J_{\text{Si(2)-F}} = 61.0$  Hz;  $J = 30.9$  Hz;  $J = 25.6$  Hz,  $J = 14.9$  Hz).

**2-Fluoro-1,2-bis(trimethylsilyl)-1,2-bis(undecamethylcyclohexasilanyl)disilanylpotassium·18-crown-6 (12).** The reaction was carried out in a manner analogous to that described above for the preparation of **3a**, using **11** (100 mg, 0.19 mmol),  $\text{KO}^t\text{Bu}$  (21 mg, 1 equiv), and 18-crown-6 (50 mg, 1 equiv). After 10 min,  $^{19}\text{F}$  NMR spectroscopy indicated that all of the starting material was consumed, and about 30% disilene adduct was formed, with the fluorosilylenoid [ $^{19}\text{F}$  NMR (toluene/ $\text{D}_2\text{O}$  capillary)  $\delta$  -274 ppm] being the main component. After 16 h, complete conversion was achieved, and **12** (92 mg, 81%) was isolated as a red oil.  $^{29}\text{Si}$  NMR ( $\text{C}_6\text{D}_6$ )  $\delta$  (ppm): 70.9 (d,  $J_{\text{Si-F}} = 340.8$  Hz); -5.3 (d,  $J = 6.6$  Hz,  $\text{SiMe}_3$ ); -20.0 ( $J = 26.0$  Hz,  $\text{SiMe}_3$ ); -34.6 to -42.6 (m,  $2 \times \text{CHS}$ ,  $-\text{SiMe}_2-$ ); -65.4 ( $J = 9.8$  Hz); -74.0 ( $J = 24.0$  Hz,  $-\text{SiMe}-$ ); -179.8 (d,  $J = 79.4$  Hz).  $^{19}\text{F}$  NMR ( $\text{C}_6\text{D}_6$ )  $\delta$  (ppm): -204.9.

**Reaction of Fluoromethylbis(trimethylsilyl)silane (13) with  $\text{KO}^t\text{Bu}$ .** To a solution of **13** (250 mg, 1.20 mmol) in THF (3 mL),  $\text{KO}^t\text{Bu}$  (135 mg, 1.20 mmol) was added. After 20 min, the solution was poured into a degassed ice-cold mixture of 0.5 M  $\text{H}_2\text{SO}_4$  and diethyl ether. The layers were separated and the aqueous layer washed twice with diethyl ether. After the combined organic layers were dried over  $\text{Na}_2\text{SO}_4$  and the solvent had been removed, *tert*-butoxymethylbis(trimethylsilyl)silane was obtained as a colorless oil (248 mg, 78%).  $^{29}\text{Si}$  NMR ( $\text{C}_6\text{D}_6$ )  $\delta$  (ppm): -2.4; -19.6.  $^1\text{H}$  ( $\text{C}_6\text{D}_6$ )  $\delta$  (ppm): 1.23 (s, 9H); 0.39 (s, 3H); 0.14 (s, 18H).  $^{13}\text{C}$  NMR ( $\text{C}_6\text{D}_6$ )  $\delta$  (ppm): 71.9; 32.2; 0.6; -1.2. When the reaction was allowed to proceed for 24 h, no fluorinated silicon compound was observed, and methylbis(trimethylsilyl)silylpotassium was the main product.  $^{29}\text{Si}$  NMR ( $\text{C}_6\text{D}_6$ )  $\delta$  (ppm): -7.6; -129.1.  $^1\text{H}$  NMR ( $\text{C}_6\text{D}_6$ )  $\delta$  (ppm): 3.50 (m, 8H, THF); 1.41 (m, 8H, THF); 0.38 (s, 18H); 0.32 (s, 3H).  $^{13}\text{C}$  NMR ( $\text{C}_6\text{D}_6$ )  $\delta$  (ppm): 67.8; 25.4; 3.5; -9.4.

**Reaction of Fluorophenylbis(trimethylsilyl)silane (14) with  $\text{KO}^t\text{Bu}$ .** To a solution of **14** (274 mg, 1.01 mmol) in THF (3 mL),  $\text{KO}^t\text{Bu}$  (114 mg, 1.01 mmol) was added. After 10 min, most of the **14** was converted to *tert*-butoxyphenylbis(trimethylsilyl)silane, which reacted over the next 10 h to give phenylbis(trimethylsilyl)silylpotassium.

Data for *tert*-butoxyphenylbis(trimethylsilyl)silane:  $^{29}\text{Si}$  NMR (toluene/ $\text{D}_2\text{O}$  capillary)  $\delta$  (ppm): -8.7; -19.4.  $^1\text{H}$  NMR ( $\text{C}_6\text{D}_6$ )  $\delta$  (ppm): 7.72 (m, 2H); 7.44 (m, 2H); 7.09 (m, 1H); 1.40 (s, 9H); 0.33 (s, 18H).

Data for phenylbis(trimethylsilyl)silylpotassium:  $^{29}\text{Si}$  NMR ( $\text{C}_6\text{D}_6$ )  $\delta$  (ppm):  $-10.1$ ;  $-97.2$ .  $^1\text{H}$  NMR ( $\text{C}_6\text{D}_6$ )  $\delta$  (ppm):  $7.73$  (d, 2H);  $6.99$  (t, 2H);  $6.80$  (t, 1H);  $3.44$  (m, 8H, THF);  $1.40$  (m, 8H, THF);  $0.47$  (s, 18H).  $^{13}\text{C}$  NMR ( $\text{C}_6\text{D}_6$ )  $\delta$  (ppm):  $157.4$ ;  $136.5$ ;  $127.5$ ;  $122.9$ ;  $67.7$ ;  $25.5$ ;  $4.3$ .

**Reaction of Fluoro-*tert*-butylbis(trimethylsilyl)silane (15) with KO<sup>t</sup>Bu.** To a solution of **15** (300 mg, 1.20 mmol) in toluene (3 mL), KO<sup>t</sup>Bu (135 mg, 1.20 mmol) and 18-crown-6 (317 mg, 1.20 mmol) were added. The solution immediately turned orange, and after 10 min, a mixture of *tert*-butylbis(trimethylsilyl)silylpotassium and 2-fluoro-1,2-di-*tert*-butyl-1,2-bis(trimethylsilyl)disilanylpotassium·18-crown-6 (**16**) was formed.

Data for *tert*-butylbis(trimethylsilyl)silylpotassium:  $^{29}\text{Si}$  NMR (toluene/ $\text{D}_2\text{O}$  capillary)  $\delta$  (ppm):  $-10.5$ ;  $-74.7$ .  $^1\text{H}$  NMR (toluene/ $\text{D}_2\text{O}$  capillary)  $\delta$  (ppm):  $3.37$  (s, 24H);  $1.32$  (s, 9H);  $0.43$  (s, 18H).

Data for **16**:  $^{29}\text{Si}$  NMR (toluene/ $\text{D}_2\text{O}$  capillary)  $\delta$  (ppm):  $65.2$  (d,  $J_{\text{Si(1)-F}} = 324.6$  Hz);  $-12.0$  (d,  $J = 24.1$  Hz);  $-21.5$  (d,  $J =$

$32.1$  Hz);  $-61.1$  (d,  $J = 52.2$  Hz).  $^1\text{H}$  NMR (toluene/ $\text{D}_2\text{O}$  capillary)  $\delta$  (ppm):  $3.37$  (s, 24H);  $1.53$  (s, 9H);  $1.48$  (s, 9H);  $0.49$  (s, 9H);  $0.45$  (s, 9H).  $^{19}\text{F}$  NMR (toluene/ $\text{D}_2\text{O}$  capillary)  $\delta$  (ppm):  $-187.6$ .

**Acknowledgment.** This study was supported by the Austrian Fonds zur Förderung der Wissenschaften (FWF) via Projects Y-120 (C.M.), P-19338 (C.M.), and P-16912 (M.F.)

**Supporting Information Available:** Synthetic details for the preparation of fluorosilanes; X-ray crystallographic information in CIF format for compounds **3a**, **3b**, **4**, and **11**; complete ref 22; and calculated structures and absolute energies of the monomers and dimers. This material is available free of charge via the Internet at <http://pubs.acs.org>.

JA805753D